Pyrene-Benzothiadiazole Based Copolymers for Application in Photovoltaic Devices

Bakhet A. Alqurashy,[a] Luke Cartwright,[a] Ahmed Iraqi,[a]* Yiwei Zhang [b] and David. G. Lidzey.[b]*

[a]Department of Chemistry, University of Sheffield, Sheffield S3 7HF, UK, E-mail: a.iraqi@sheffield.ac.uk.

[b]Department of Physics and Astronomy, University of Sheffield, Sheffield S3 7RH, UK, E-mail: d.g.lidzey@sheffield.ac.uk

Abstract

The preparation and characterisation of four narrow band gap pyrene-benzothiadiazole based alternating copolymers is presented. An investigation of the impact of attaching different solubilising groups to the pyrene repeat units on the optical, electrochemical and thermal properties of the resulting materials was undertaken along with studies on the aggregation of polymer chains in the solid state. Unsurprisingly, polymers which had the smaller 2-ethylhexyl chains attached to the pyrene units (**PP$_{EH}$-DTBT** and **PP$_{EH}$-DTffBT**) displayed lower molecular weights relative to polymers with larger 2-hexyldecyl substituents (**PP$_{HD}$-DTBT** and **PP$_{HD}$-DTffBT**). Despite this, the 2-ethylhexyl substituted polymers displayed narrower optical band gaps relative to their analogous 2-hexyldecyl substituted polymers. Of all polymers synthesised, **PP$_{EH}$-DTBT** displayed the lowest optical band gap (1.76 eV) in the series. All polymers display degradation temperatures in excess of 300°C. Polymers with smaller alkyl chains on the pyrene units display shallower HOMO levels which could be due to increased intramolecular charge transfer between the donor and acceptor units. Preliminary investigations on bulk heterojunction solar cells with a device structure ITO/PEDOT:PSS/Polymer:PC$_{70}$BM/Ca/Al were undertaken. Polymer/PC$_{70}$BM blend ratios of 1/3 were used in these studies and have indicated that **PP$_{EH}$-DTBT** displayed the highest efficiency with a PCE of 1.86 %.

Introduction

Organic semiconductors have gained a tremendous amount of attention from researchers in recent years owing to the advantages they possess over their inorganic counterparts. These advantages include: high absorption coefficients, non-toxic and recyclable materials and can be

manufactured on lightweight, flexible substrates *via* low-cost solution processing methods. These unique electrical and optical properties make organic semiconductors promising candidates for use in organic photovoltaic cells (OPV), organic light emitting diodes (OLEDs) and organic field effects transistors (OFETs).[1,2,3,4]

Bulk heterojunction (BHJ) photovoltaic devices based on conjugated polymers as p-type organic semiconductors, and fullerene derivatives as n-type organic semiconductors, have been intensively studied in recent years. This has resulted in the efficiency of OPV BHJ devices rising from less than 1 % to over 10 %. The high rise in efficiencies can be attributed to the development of conjugated polymers and the improvement in the morphology of the photoactive layer of BHJ solar cells.[5,6,7] Previous literature reports have shown that BHJ solar cells fabricated from donor-acceptor (D-A) conjugated polymers yield the best efficiencies. In the D-A approach, an electron-poor acceptor unit is copolymerised with an electron-rich donor unit. A fraction of electronic charge is transferred between the electron-rich and electron-poor units along polymer chains, leading to intramolecular charge transfer (ICT) and a narrow optical band gap; allowing the polymer to absorb large portions of light from the visible spectrum.[8,9,10]

Benzothiadiazole (**BT**) based copolymers have received a large amount of attention from the academic community. High efficiencies have been reported for BHJ solar cells fabricated from benzothiadiazole based D-A copolymers.[9] Recently, Liu *et al* reported the synthesis of highly efficient BHJ solar cells based on benzothiadiazole-thiophene alternate copolymers.[11] Efficiencies of 10.8% were achieved when the polymer, **PffBT4T-2OD**, was blended with the fullerene acceptor **TC$_{71}$BM**. High efficiencies were still achieved when thick-film (250-300 nm) polymer solar cells were fabricated. Other efficient **BT** based polymers include **BDT-DTBTff** synthesised by You and co-workers which achieved an efficiency of 7.2 % when fabricated into BHJ solar cells.[10,12,13,14]

Polycyclic aromatic hydrocarbons (PAHs) have found widespread use in OPV and OLED devices.[15] Compared to other PAHs such as naphthalene and anthracene,[16,17,18] pyrene-based conjugated polymers have received little attention from researchers. Pyrene is a planar, symmetrical, electron rich unit that possesses an extended π-conjugated system. Thus, pyrene molecules may exhibit strong π-π stacking and a high degree of crystallinity which could promote charge carrier mobility. Furthermore, the electron rich nature of pyrene means that the

pyrene-unit can be polymerised with electron-deficient units forming the advantageous D-A arrangement discussed above. The pyrene unit can be polymerised through the 2,7-poitions.[19,20] Furthermore, the optical and electronic properties of pyrene units can be altered by functionalising the 4,5,9,10-positions of pyrene with different substituents. Yang and co-workers synthesised a series pyrene-diketopyrrolopyrrole based copolymers for use in OFETs. **P(DTDPP-*alt*-(2,7)PY)** displayed a narrow optical band gap of 1.65eV and hole mobilities of 0.23 cm^2 V^{-1} s^{-1}.[21] Hwang *et al* reported the synthesis of pyrene based alternate copolymers.[22] BHJ solar cells fabricated from these polymers displayed efficiencies up to 5.04%. They synthesised a terpolymer, **PBDTDTBT** that comprised carbazole, benzothiadiazole and pyrene repeat units. **PBDTDTBT** was compared to the well-studied polymer, **PCDTBT**. The researchers found that **PBDTDTBT** displayed higher charge transport abilities when compared to **PCDTBT**, a consequence of incorporating pyrene units. Solar cells based on **PBDTDTBT** displayed efficiencies of 3.34 %, which is higher than that of solar cells fabricated from **PCDTBT** using similar conditions. Furthermore, the introduction of pyrene resulted in the polymers displaying higher open circuit voltages.[22]

Herein, we report the preparation of four D-A polymers comprising pyrene-benzothiadiazole repeat units. Poly(4,5,9,10-tetrakis((2-hexyldecyl)oxy)-pyrene-2,7-diyl-alt-(4,7-dithiophen-2-yl)-2',1',3'-benzothiadiazole-5,5-diyl] **(PP$_{HD}$-DTBT)**, poly(4,5,9,10-tetrakis((2-hexyldecyl)oxy)pyrene-2,7-diyl-alt-(5,6-difluoro-4,7-di(thiophen-2-yl)-2',1',3'-benzothiadiazole-5,5-diyl] **(PP$_{HD}$-DTffBT)**, poly(4,5,9,10-tetrakis((2-ethylhexyl)oxy)pyrene-2,7-diyl-alt-(4,7-dithiophen-2-yl)-2',1',3'-benzothiadiazole-5,5-diyl] **(PP$_{EH}$-DTBT)** and poly-4,5,9,10-tetrakis((2-ethylhexyl)oxy)pyrene-2,7-diyl-alt-(5,6-difluoro-4,7-di(thiophen-2-yl)-2',1',3'-benzothiadiazole-5,5-diyl] **(PP$_{EH}$-DTffBT)** were synthesised by Stille polymerisation (Scheme 1). The properties of the polymers were investigated and their performance in BHJ photovoltaic devices was assessed. Polymers that had smaller alkyl chains attached to the pyrene unit displayed narrower optical band gaps, shallower HOMO levels and improved π-π stacking in solid state. BHJ solar cells fabricated from **PP$_{HD}$-DTBT**, **PP$_{EH}$-DTBT**, **PP$_{HD}$-DTffBT** and **PP$_{EH}$-DTffBT** displayed efficiencies of 0.98, 1.86, 0.66 and 0.83 %, respectively.

Results and Discussion

Polymer Synthesis: The preparation of monomers 2,7-dibromo-4,5,9,10-tetrakis((2-hexyldecyl)oxy)pyrene (**4**) and 2,7-dibromo-4,5,9,10-tetrakis((2-ethylhexyl)oxy)pyrene (**5**) is depicted in Scheme 2. Both pyrene monomers were synthesised starting from the commercially available pyrene. The pyrene was oxidised at the 4,5,9,10-positions using $RuCl_3.xH_2O$ and $NaIO_4$. Intermediate **2** was brominated at the 2,7-positions using N-bromosuccinimide (NBS) to yield **3**. The final step of the synthesis involved attaching the solubilising alkyl chains to the 4,5,9,10 positions to afford **4** and **5** respectively. 4,7-Bis(5-(trimethylstannyl)thiophen-2-yl)benzo[c] [1,2,5]thiadiazole (**DTBT**) and 5,6-difluoro-4,7-bis(5-(trimethyl stannyl)thiophen-2-yl)benzo[c][1,2,5]thiadiazole (**DTffBT**) were prepared according to literature procedures.[1,23]

All polymers were prepared *via* Stille coupling using Pd(OAc)$_2$ and tri(*o*-tolyl)phosphine as the catalyst and toluene as the solvent. All polymerisations, with the exception of **PP$_{EH}$-DTffBT**, were conducted over 48 hours. Polymerisation of **PP$_{EH}$-DTffBT** was stopped after 2 hours, as after this time polymer precipitation was observed as a result of its lower solubility. The crude polymers were purified *via* Soxhlet extraction using methanol, acetone, hexane, toluene and chloroform. The methanol, acetone and hexane fractions,removed catalyst residues, inorganic impurities and low molecular weight oligomers/polymers. The toluene fractions were collected for **PP$_{HD}$DTBT** and **PP$_{HD}$-DTffBT**. In contrast, the chloroform fraction was collected for **PP$_{EH}$-DTBT**, and **PP$_{EH}$-DTffBT**, a consequence of the smaller alkyl chain on the pyrene repeat units which provide lower solubility in toluene fractions on Soxhlet extraction. The number-average molecular weights (M_n) and weigh-average molecular weighs (M_w) were determined *via* gel permeation chromatography (GPC) at 140°C using 1,2,4-trichlorobenzene as the eluent. A series of polystyrene standards were used as the internal standards and the results are outlined in Table 1. Unsurprisingly, polymers that are substituted with the short 2-ethylhexyl chains displayed lower molecular weights relative to polymers that are substituted with the larger 2-hexyldecyl alkyl chains. Clearly, the incorporation of larger alkyl chains on the pyrene units inhibits intermolecular interactions between polymer chains aiding the formation of processable polymer materials with higher molecular weight. Interestingly, **PP$_{EH}$-DTffBT** displayed a lower M_n

(5,300 Da) relative to its non-fluorinated analogue, **PP$_{EH}$-DTBT** (12,800 Da). Previous literature has shown that the incorporation of fluorine on the benzothiadiazole-unit results in stronger π-π stacking interactions and aggregation of polymers chains, which limits the final molecular weight of the polymer.[23,24] However, **PP$_{HD}$-DTffBT** (20,700 Da) did not display a lower M_n relative to its non-fluorinated analogue, **PP$_{HD}$-DTBT** (20,500 Da). It is speculated that the large 2-hexyldecyl chains are long enough to break these additional interactions, in solution, facilitating the formation of a high molecular weight material.

UV-vis absorption spectroscopy: The optical properties of all polymers were investigated by UV-vis spectroscopy in dilute chloroform solutions (Figure 1a) and film states (Figure 1b). The optical band gaps of the polymers were calculated from their onsets of absorption in films. The data is summarised in Table 1. All UV-vis spectra display two main absorption bands. The band at shorter wavelengths can be attributed to π-π* transitions whereas the absorption bands at longer wavelengths can be attributed to intramolecular charge transfer (ICT) between the electron-rich pyrene units flanked by thiophene rings and the electron-deficient benzothiadiazole units. In solutions, the ICT absorption maxima are located at 531, 538, 526 and 521 nm for **PP$_{HD}$-DTBT**, **PP$_{EH}$-DTBT**, **PP$_{HD}$-DTffBT** and **PP$_{EH}$-DTffBT**, respectively. When cast into films these maxima are red-shifted to 571, 585, 562 and 564 nm for **PP$_{HD}$-DTBT**, **PP$_{EH}$-DTBT**, **PP$_{HD}$-DTffBT** and **PP$_{EH}$-DTffBT**, respectively. The bathochromic shifts can be attributed to the polymers adopting more planar conformations in the solid state, which extends the electronic conjugation along the backbone of polymers. When cast into films, polymers with shorter alkyl chains, **PP$_{EH}$-DTBT** and **PP$_{EH}$-DTffBT**, display more red-shifted absorption maxima relative to their analogous polymers, **PP$_{HD}$-DTBT** and **PP$_{HD}$-DTffBT**. Furthermore, all fluorinated polymers display a hypsochromic shift relative to their non-fluorinated polymers. This phenomenon has been reported in previous literature.[24]

A very small shoulder appeared at shorter wavelength for all polymers. This was located at 346 and 348 nm in solution and film states, respectively. This phenomenon has been observed in most donor-acceptor conjugated polymers containing DTBT units.[10] The UV-vis spectra of **PP$_{HD}$-DTffBT** and **PP$_{EH}$-DTffBT** both display a small shoulder peak at ~500 nm in solid state. **PP$_{EH}$-DTBT** also displays a shoulder peak in this region, however, it is not as pronounced. Interestingly, this shoulder peak is completely absent in **PP$_{HD}$-DTBT**. Previous work has

speculated that the incorporation of fluorine substituents yield additional intermolecular interactions between fluorine substituents with neighbouring aromatic chains. Thus, the polymer adopts a more planar conformation with improved stacking between polymer chains.[24] It is possible that the short 2-ethylhexyl chains in **PP$_{EH}$-DTBT** allow a similar π-π stacking of polymer chains to occur all be it to a much reduced level. In contrast, the large alkyl chains attached to **PP$_{HD}$-DTBT** disrupt intermolecular interactions resulting in a higher degree of structural and electronic disorder which is displayed in the broad, ill-resolved absorption bands.

The optical band gaps of **PP$_{HD}$-DTBT**, **PP$_{EH}$-DTBT**, **PP$_{HD}$-DTffBT** and **PP$_{EH}$-DTffBT** were estimated to be 1.77, 1.74, 1.84 and 1.81 eV, respectively. **PP$_{EH}$-DTBT** and **PP$_{EH}$-DTffBT** displayed narrower optical band gaps relative to their analogous polymers, **PP$_{HD}$-DTBT** and **PP$_{HD}$-DTffBT**. The rational for this can be linked to the size of the solubilising chain attached to the pyrene donor-units on the respective polymers. It is also noted that the band gaps of the non-fluorinated polymers (**PP$_{HD}$-DTBT** and **PP$_{EH}$-DTBT**) are narrower than those of their fluorinated analogues (**PP$_{HD}$-DTffBT** and **PP$_{EH}$-DTffBT**) as a consequence of deeper HOMO levels in the fluorinated polymers (see below).

PP$_{HD}$-DTBT, **PP$_{EH}$-DTBT**, **PP$_{HD}$-DTffBT** and **PP$_{EH}$-DTffBT** are analogous polymers to the benzothiadiazole-anthracene based polymer **PPATBT** synthesised by Almeataq *et al.*[18], which uses an anthracene functionalised with 4-dodecyloxybenzene as the donor polyaromatic hydrocarbon unit, instead of pyrene and which has an optical band gap of 1.84 eV, or to the fluorinated benzothiadiazole-anthracene based polymer **PTATffBT** synthesised by Cartwright and co-workers,[25] which has a band gap of 1.92 eV. It is speculated that the additional cyclic aromatic ring in pyrene units for polymers described in this study extends the electron conjugation, yielding more planar polymer backbones which improves π-π stacking in the solid state.

Thermal Properties: Thermogravimetric analysis (TGA) was used to investigate the thermal properties of the polymers synthesised within this report. All polymers display degradation temperatures (5% weight loss) in excess of 320°C. **PP$_{HD}$-DTBT**, **PP$_{EH}$-DTBT, PP$_{HD}$-DTffBT** and **PP$_{EH}$-DTffBT** displayed degradation temperatures of 328, 322, 328 and 320°C, respectively. All initial weight losses can be attributed to the loss of alkyl chains from the pyrene donor-unit. **PP$_{EH}$-DTBT** and **PP$_{EH}$-DTffBT** both display second weight loss peaks at 530 and 513 °C,

respectively. This second weight loss peak corresponds to degradation of the polymer backbone. Interestingly, this second weight loss peak is absent in both **PP_{HD}-DTBT** and **PP_{HD}-DTffBT**. It is speculated that the larger 2-hexyldecyl chain is significantly less volatile, when combusted, relative to the 2-ethylhexyl chain. Thus, as **PP_{HD}-DTBT** and **PP_{HD}-DTffBT** degrade a char layer is formed over the virgin polymer which acts as a thermal insulator owing to its low thermal conductivity. Consequently, the char layer reduces the heat flux reaching the virgin polymer. Furthermore, as the surface temperature of the char increases there will be a significant increase in re-radiation losses. Both of these processes retard thermal degradation of the polymer.[26]

Cyclic Voltammetry: Cyclic voltammetry was used to characterise the frontier energy levels of **PP_{HD}-DTBT**, **PP_{EH}-DTBT**, **PP_{HD}-DTffBT** and **PP_{EH}-DTffBT**. Studies were carried out on drop-cast polymer films in acetonitrile and tetrabutylammonium perchlorate as electrolyte (Figure 3). The onsets of oxidation and reduction were used to assess the HOMO and LUMO energy levels of the polymers. The values of these (*vs. vacuum*) along with the electrochemical energy band gaps calculated from the difference of their HOMO and LUMO levels are shown in Table 1. All fluorinated polymers display deeper HOMO levels relative to their non-fluorinated counterparts; a consequence of attaching electron withdrawing substituents to the benzothiadiazole unit. This phenomenon has been observed in previous literature.[27,28] It is speculated that the lower HOMO levels of fluorinated polymers should result in a higher open circuit voltage (V_{oc}) in photovoltaic devices. Furthermore, the polymers should display better oxidative stability relative to their non-fluorinated counterparts. The HOMO/LUMO levels of **PP_{HD}-DTffBT** and **PP_{EH}-DTffBT** were positioned at -5.60/-3.28 eV and -5.53/-3.55 eV, respectively. Clearly, the LUMO level of **PP_{EH}-DTffBT** is positioned further from the *vacuum* level than that of **PP_{HD}-DTffBT**. It is speculated that this is a consequence of attaching larger alkyl chains to the pyrene-units which lead to lower electronic delocalisation. The shallower HOMO level of **PP_{EH}-DTffBT** is a consequence of attaching shorter 2-ethyl hexyl chains to the pyrene-units. It is hypothesised that the shorter alkyl chains in **PP_{EH}-DTffBT** facilitate improved intermolecular interactions and a more planar polymer backbone which facilitates intramolecular charge transfer between the electron deficient and electron donating units. This phenomenon is repeated in the non-fluorinated polymers **PP_{HD}-DTBT** and **PP_{EH}-DTBT**. Their HOMO/LUMO levels are positioned at -5.50/-3.28 eV and -5.45/-3.55, respectively. The electrochemical band gaps of **PP_{HD}-DTBT**, **PP_{EH}-DTBT**, **PP_{HD}-DTffBT** and **PP_{EH}-DTffBT** were estimated to be

2.22, 1.90, 2.32 and 1.98 eV, respectively. The electrochemical band gaps are significantly larger than the optical band gaps. Previous literature has shown this is a consequence of an additional interfacial barrier between the polymer films and electrode surface.[29]

Powder X-ray diffraction (PXRD): The molecular organisation of **PP$_{HD}$-DTBT**, **PP$_{EH}$-DTBT**, **PP$_{HD}$-DTffBT** and **PP$_{EH}$-DTffBT** in the solid state were probed *via* powder X-ray diffraction patterns (PXRD) (Figure 4). The PXRD pattern of **PP$_{HD}$-DTBT** and **PP$_{HD}$-DTffBT** both display broad, diffuse features in the wide angle region at 20.7° and a poorly resolved peak in the small angle region at 3.67°. These correspond to a π-π stacking distance of 4.29 Å and a lamellar distance of ~24.0 Å, respectively.[24] Previous literature reports have shown that fluorination of the benzothiadiazole unit yields a decrease in the π-π stacking distance.[23,24,25] **PP$_{HD}$-DTffBT** does not follow this reported trend. It is speculated that the large 2-hexyldecyl negate the effects fluorination has on the π-π stacking properties of the polymer in the solid state. Thus, **PP$_{HD}$-DTffBT** possesses the same number and extent of intermolecular interactions as **PP$_{HD}$-DTBT**. **PP$_{EH}$-DTBT** and **PP$_{EH}$-DTffBT** display lamellar stacking distances of 18.0 and 17.9 Å, respectively, and π-π stacking distances of 3.81 and 3.59 Å, respectively. Unsurprisingly, polymers that have 2-ethylhexyl chains attached to the pyrene-unit possess smaller lamellar stacking distances relative to polymers that have 2-hexyldecyl chains attached to the pyrene unit. The smaller π-π stacking distance of **PP$_{EH}$-DTffBT**, relative to **PP$_{EH}$-DTBT**, can be attributed to the incorporation of fluorine. Previous literature has reported this phenomenon.[24] The smaller stacking distance and more resolved peaks in **PP$_{EH}$-DTffBT** relative to **PP$_{EH}$-DTBT** suggest the polymer adopts a more crystalline structure in the solid state. [23,24,25]

Photovoltaic properties: Preliminary studies on the photovoltaic properties of the four polymers were undertaken. Bulk heterojunction solar cells were fabricated with a device architecture of Glass/ITO/PEDOT:PSS/Polymer:PC$_{70}$BM/Ca/Al using a mixture of Polymer:PC$_{70}$BM in a weight ratio of 1:3 in chlorobenzene as the processing solvent. A detailed device fabrication is outlined in the experimental section. The current density-voltage (J-V) characteristic curves from these devices are displayed in Figure 5. The device parameters are depicted in Table 2. The V_{oc} values for polymers with 2-hexyldecyl substituents **PP$_{HD}$-DTBT** and **PP$_{HD}$-DTffBT** are found to be higher (0.90 and 0.93 V respectively) than those of polymers with the smaller 2-ethylhexyl substituents **PP$_{EH}$-DTBT** and **PP$_{EH}$-DTffBT** (0.74 and 0.79 V respectively). This can be partly

explained with their deeper HOMO energy levels (-5.50 and -5.60 eV for **PP$_{HD}$-DTBT** and **PP$_{HD}$-DTffBT** respectively *vs.* -5.45 and -5.53 eV for **PP$_{EH}$-DTBT** and **PP$_{EH}$-DTffBT** respectively). All polymers exhibit modest efficiencies. **PP$_{EH}$-DTBT** boasted the highest efficiency in this series of polymers with a PCE of 1.86 %, FF of 60.58 % and a J$_{sc}$ of 4.14 mA/cm^2. In contrast, the equivalent polymer, which has the larger 2-hexyldecyl chains attached to the pyrene units **PP$_{HD}$-DTBT** demonstrated a PCE of 0.98 %, a FF of 45.81 % and a J$_{sc}$ of 2.38 mA cm^{-2}. The higher J$_{sc}$ and FF of **PP$_{EH}$-DTBT**, relative to those of **PP$_{HD}$-DTBT**, are presumably a result of the smaller 2-ethylhexyl substituents attached to its pyrene repeat units. As shown from the X-ray diffraction studies, the smaller alkyl chains yield a smaller amount of steric hindrance which should improve the packing of polymer chains in the photoactive layer of the photovoltaic device. The improved stacking should yield improved charge mobility and extraction in photovoltaic devices fabricated from **PP$_{EH}$-DTBT**, relative to those fabricated form **PP$_{HD}$-DTBT**. It is worth noting that a similar phenomenon is observed when comparing the two analogous polymers, **PP$_{HD}$-DTffBT** and **PP$_{EH}$-DTffBT**.

Conclusions

Four novel pyrene-benzothiadiazole alternating copolymers were synthesised *via* Stille coupling. 2-Hexyldecyl or 2-ethylhexyl chains were attached to the pyrene moiety to assess the impact this had on the properties of the resulting polymers. All polymers displayed good solubility in common organic solvents. GPC analysis showed that incorporation of 2-hexyldecyl chains allowed polymers to be obtained with higher molecular weights and enabled the additional intermolecular interactions brought about by fluorination of the benzothiadiazole moieties along polymer chains to be overcame. Thus, **PP$_{HD}$-DTBT** and **PP$_{HD}$-DTffBT** displayed similar number average molecular weights. **PP$_{EH}$-DTBT** and **PP$_{EH}$-DTffBT** displayed narrower optical band gaps relative to their analogous polymers, **PP$_{HD}$-DTBT** and **PP$_{HD}$-DTffBT**. Additionally, **PP$_{EH}$-DTBT** and **PP$_{EH}$-DTffBT** displayed shallower HOMO levels relative to their analogous polymers. Both of these phenomena can be attributed to shorter alkyl chains being attached to the pyrene donor. The shorter alkyl chains are less disrupting to intermolecular interactions when compared to the larger alkyl chains. Thus, polymers bearing shorter alkyl chains adopt a more planar structure in the solid state. This hypothesis was confirmed with powder X-ray diffraction

studies which showed polymers bearing 2-ethylhexyl chains possessed smaller lamellar and π-π stacking distances relative to polymers bearing 2-hexyldecyl chains. Bulk heterojunction solar cells were fabricated from all polymers. $PC_{70}BM$ was used as the electron acceptor and blends of polymer:$PC_{70}BM$ ratios of 1:3 were investigated. All polymers displayed modest efficiencies. **PP$_{EH}$-DTBT** displayed the highest efficiency with a PCE of 1.86 %. Further studies into the optimisation of the photovoltaic properties of these promising materials are underway.

Experimental

Materials: All materials were purchased from commercial suppliers and used as received, unless otherwise stated. Toluene was dried and distilled over sodium under an inert argon atmosphere. Acetonitrile was dried and distilled over phosphorous pentoxide and stored under an inert atmosphere with molecular sieves (3 Å). Pyrene-4,5,9,10-tetraone (**2**),[30,31] 2,7-dibromopyrene-4,5,9,10-tetraone (**3**) and 2,7-dibromo-4,5,9,10-tetrakis((2-hexyldecyl) oxy)pyrene (**4**)[20] were synthesised according to literature procedures.

Measurements: [1]H and ^{13}C nuclear magnetic resonance (NMR) spectra were recorded on a Bruker AV 400 (400 MHz) using chloroform-d ($CDCl_3$). ^{1}H-NMR of the polymers were recorded on Bruker Avance III HD 500 (500 MHz) spectrometer at 100°C using 1,2-dideutrotetrachloroethance as the solvent. Coupling constants are given in Hertz (Hz). Carbon, hydrogen, nitrogen and sulphur elemental analysis was performed on a Perkin Elmer 2400 series 11 CHNS/O analyser. Analysis of halides was undertaken using the Schöniger flask combustion method. GPC analysis was conducted on polymer solutions using 1,2,4-trichlorobenzene at 140°C as the eluent. Polymer samples were spiked with toluene as a reference. GPC curves were obtained using a Viscotek GPCmax VE2001 GPC solvent/sample module and a Waters 410 Differential Refractometer, which was calibrated using a series of narrow polystyrene standards (Polymer Laboratories). TGA curves were obtained using a Perkin Elmer TGA-1 Thermogravimetric Analyser at a scan rate of 10°C min^{-1} under an inert nitrogen atmosphere. Powder X-ray diffraction samples were recorded on a Bruker D8 advance diffractometer with a CuKα radiation source (1.5418 Å, rated as 1.6 kW). The scanning angle was conducted over the range 2-40°. UV-visible absorption spectra were recorded using a Hitachi U-2010 Double Bean UV/Visible Spectrophotometer. Polymer solutions were made using chloroform and measured

using quartz cuvettes (path length = 1×10^{-2} m). Thin films, used for absorption spectra were prepared by drop-casting solutions onto quartz plates using 1 mg cm^{-3} polymer solutions that were prepared with chloroform. Cyclic voltammograms were recorded using a Princeton Applied Research Model 263A Potentiostat/Galvanostat. A three electrode system was employed comprising a Pt disc, platinum wire and Ag/Ag$^+$ as the working electrode, counter electrode and reference electrode, respectively. Measurements were conducted in a tetrabutylammonium perchlorate acetonitrile solution (0.1 mol dm^{-3}) on polymer films that were prepared by drop casting polymer solution. Ferrocene was employed as the reference redox system; in accordance with IUPAC's recommendations. The energy level of Fc/Fc$^+$ was assumed at -4.8 eV to vacuum. The half-wave potential of Fc/Fc$^+$ redox couple was found to be 0.08 V *vs.* Ag/Ag$^+$ reference electrode. The HOMO energy levels of polymers were estimated by equation: $E_{HOMO} = -(4.8 - E_{1/2, Fc,Fc+} + E_{ox, onset})$. $E_{ox, onset}$ is the onset oxidation potential relative to the Ag/Ag$^+$ reference electrode. The LUMO energy levels of polymers were calculated using the equation: $E_{LUMO} = -(4.8 - E_{1/2, Fc,Fc+} + E_{red, onset})$. $E_{red,onset}$ is the onset reduction potential relative to the Ag/Ag+ reference electrode.

Fabrication and testing of BHJ polymer solar cells: The polymers and PC$_{70}$BM were dissolved in chlorobenzene, and were then put on a hot plate held at 70 °C overnight with stirring to allow dissolution. The polymer:fullerene blend ratios were 1:3. Photovoltaic devices were fabricated onto pre-patterned ITO glass substrates (20 ohms per square) that were supplied by Ossila Limited. The ITO/glass substrates were first cleaned by sonication in dilute NaOH followed by IPA. A 30 nm thick PEDOT:PSS layer was spin-coated onto the ITO/glass substrates. These were then transferred to a hot-plate held at 120 °C for 10 minutes before being transferred to a nitrogen glove-box. All active layers were spin cast onto the glass/ITO/PEDOT:PSS substrate. The devices were then transferred into a thermal evaporator for deposition of a cathode (5 nm of calcium followed by a 100 nm of aluminium evaporated at a base pressure of $\sim 10^{-7}$ mbar). The cathode was deposited through a shadow-mask producing a series of independent pixels. Devices were encapsulated using a glass slide and epoxy glue before testing. PCEs were determined using a Newport 92251A-1000 AM 1.5 solar simulator. An NREL calibrated silicon cell was used to calibrate the power output to 100 mW cm^{-2} at 25 °C. An aperture mask having an area of 2.06 mm^2 was placed over devices to define the test area.

EQE values were determined over the wavelength range of interest by comparing the photocurrent of the OPV cell to a reference silicon photodiode having a known spectral response.

Preparation of monomers and polymers:

2,7-Dibromo-4,5,9,10-tetrakis((2-ethylhexyl)oxy)pyrene (5): 2,7-dibromopyrene-4,5,9,10-tetraone (1.5 g, 3.57 mmol), $Na_2S_2O_4$ (7.25 g, 41.66 mmol), n-Bu_4NBr (1.44 g, 4.46 mmol), H_2O (12 mL) and THF (24 mL) were placed in a round bottom flask and stirred for 10 minutes at 25°C. Once the time had elapsed, 2-ethylhexyl bromide (4.54 g, 23.5 mmol) and aq. KOH (12 mL of 8.0 M aqueous solution, 96 mmol) were added to the mixture. The mixture was stirred for 5 hours at 70 °C. Upon completion, the reaction was quenched with brine. The crude material was extracted with THF. The organic layer was washed with brine (3 x 100 mL). The organic layer was separated, dried ($MgSO_4$) and the solvent removed *in vacuo*. The crude material was purified *via* silica gel column chromatography using petroleum ether as the eluent to yield 2,7-dibromo-4,5,9,10-tetrakis((2-ethylhexyl)oxy)pyrene as yellow oil (1.8 g, 2.06 mmol, 46.26 %).[34] ^{1}H NMR (400 MHz, CDCl$_3$): (δ_H/ppm) 8.54 (s, 4H), 4.19 (d, J = 6.0 Hz, 8H), 2.00-1.89 (m, 4H), 1.80-1.37 (m, 32H), 1.06 (t, J = 7.31 Hz, 12H), 0.98 (t, J = 6.95 Hz, 12H). ^{13}C NMR (400 MHz, CDCl$_3$): (δ_C/ppm) 144.06, 130.18, 121.90, 121.13, 118.95, 40.75, 30.59, 29.17, 23.91, 23.18, 14.12, 11.22 GC-MS: mass calcd. for $C_{48}H_{72}Br_2O_4$ 872.37, found 872.5. Elem. Anal. Calcd. for $C_{80}H_{136}Br_2O$: C 66.05, H 8.31, Br 18.31; found C 66.23, H 8.22, Br 18.42.

2,7-Dibromo-4,5,9,10-tetrakis((2-hexyldecyl)oxy)pyrene (4): The titled product was synthesised as described previously in the preparation of **5**. The product was obtained as colourless oil (0.400 g, 0.30mmol, 50.66%).[34] ^{1}H NMR (400 MHz, CDCl$_3$): (δ_H/ppm) 8.54 (s, 4H), 4.18 (d, J = 6.06 Hz, 8H), 2.02-1.93 (m, 4H), 1.72-1.61 (m, 8H); 1.60-1.5 (m, 12H), 1.48-1.22 (m, 76H), 0.91 (t, J = 6.65 Hz, 24H). ^{13}C NMR (400 MHz, CDCl3): (δ_C/ppm) 143.99, 130.16, 121.89, 121.13, 118.89, 39.33, 31.94, 31.45, 30.21, 29.86, 29.70, 29.41, 27.00, 26.96, 22.74, 22.70, 14.12. GC-MS: mass calcd. for $C_{80}H_{136}Br_2O_4$ 1321, found 1321.2. Elem. Anal. Calcd. for $C_{80}H_{136}Br_2O$: C 72.70, H 10.37, Br 12.09; found C 73.22, H 10.47, Br 11.98.

Poly(4,5,9,10-tetrakis((2-hexyldecyl)oxy)-pyrene-2,7-diyl-alt-(4,7-dithiophen-2-yl)- 2',1',3'-benzothiadiazole-5,5-diyl] (PP$_{HD}$-DTBT): A mixture of 2,7-dibromo-4,5,9,10-tetrakis((2-hexyldecyl)oxy)pyrene (**5**) (160 mg, 0.12 mmol), 4,7-bis(5-(trimethylstanyl)thiophene-2-yl)benzo[c][1,2,5]thiadiazole (75 mg, 0.12 mmol), Pd(OAc)$_2$ (2.00 mg, 8.9 μmol) and tri(*o*-tolyl)phosphine (5.38 mg, 17.7 μmol) were placed in a one neck round bottom flask and placed under an inert argon atmosphere. Anhydrous toluene (10 mL) was added, the system was degassed and placed under an inert argon atmosphere. The reaction was heated to 100°C and left to stir for 48 hours. Upon completion, the reaction was allowed to cool to room temperature. 2-(Tributylstannyl)thiophene (11.7 μL, 0.037 mmol) was added, the system was degassed and the solution refluxed for 1 hour. Upon completion, the reaction was cooled to room temperature and 2-bromothiophene (45.1 mg, 0.28 mmol) was added. The reaction vessel was degassed again and the solution refluxed for a further 1 hour. Upon completion, the reaction was cooled to room temperature. Chloroform (250 mL) was then added to the reaction mixture followed by addition of an ammonium hydroxide solution (28% in H$_2$O, 40 mL) and the mixture was stirred at 60°C for 3 hour. The mixture was cooled and the organic phase was separated and washed with water (5 x 100 mL). The organic phase was collected, concentrated to 40 mL *in vacuo* and precipitated in methanol (300 mL). The solids were filtered through a membrane and subjected to Soxhlet extraction in turn with methanol, acetone, hexane and toluene. The toluene fraction was concentrated *in vacuo* and precipitated in methanol. The precipitate was stirred overnight. The pure polymer was filtered through a membrane filter and collected as a dark purple solid (65 mg, 37 %). GPC toluene fraction: M_n = 20,500 Da; M_w = 30,200 Da; PDI = 1.47. ^{1}H NMR (500 MHz, C$_2$D$_2$Cl$_4$, 100°C): (δ$_H$/ppm) 8.83 (s, 4H), 8.35 (br.d, 2H), 8.00 (br.s, 2H), 7.80 (br.d, 2H), 4.30 (br.d, 8H), 2.20-2.00 (m, 4H), 1.90-1.75 (m, 4H), 1.75-1.20 (m, 90H), 0.90 (br.t, 24H). Elem. Anal. Calcd. for C$_{94}$H$_{142}$N$_2$O$_4$S$_3$: C 77.20, H 9.90, N 1.90, S 6.58. Found: C 75.49, H 9.24, N 1.98, S 8.12.

Poly(4,5,9,10-tetrakis((2-hexyldecyl)oxy)pyrene-2,7-diyl-alt-(5,6-difluoro-4,7-di(thiophen-2-yl)-2',1',3'-benzothiadiazole-5,5-diyl] (PP$_{HD}$-DTffBT): The titled product was synthesised as described previously in the preparation of **PP$_{HD}$-DTBT**. The product was obtained as a dark purple solid (115 mg, 64 %). GPC toluene fraction: M_n = 20,700 Da; M_w = 40,400 Da; PDI = 1.95. ^{1}H NMR (500 MHz, C$_2$D$_2$Cl$_4$, 100°C): (δ$_H$/ppm) 8.86 (br.s, 4H), 8.50 (br.d, 2H), 7.83 (br.d, 2H), 4.30 (br.d, 8H), 2.20-2.00 (m, 4H), 1.90-1.75 (m, 4H), 1.75-1.20 (m, 90H), 0.90 (br.t, 24H).

Elem. Anal. Calcd. for $C_{94}H_{142}F_2N_2O_4S_3$: C 75.35, H 9.55, N 1.87, S 6.41. Found C 72.13, H 8.90, N 2.38, S 8.02.

Poly(4,5,9,10-tetrakis((2-ethylhexyl)oxy)pyrene-2,7-diyl-alt-(4,7-dithiophen-2-yl)-2',1',3'-benzothiadiazole-5,5-diyl] (PP$_{EH}$-DTBT): The titled product was synthesised as described previously in the preparation of **PP$_{HD}$-DTBT**. The product was obtained as a dark purple solid (38 mg, 35 %). GPC chloroform fraction: M_n = 12,800 Da; M_w = 20,000 Da; PDI = 1.56. ^{1}H NMR (500 MHz, $C_2D_2Cl_4$, 100°C): (δ_H/ppm) 8.80 (br.s, 4H), 8.27 (br.d, 2H), 8.00 (br.s, 2H), 7.73 (br.d, 2H), 4.3 (br.d, 8H), 2.05 (m, 4H), 1.94-1.27 (m, 32H), 1.14 (br.t, 12H), 0.98 (t, 12H). Elem. Anal. Calcd. for $C_{62}H_{78}N_2O_4S_3$: C 73.62, H 7.77, N 2.77, S 9.51. Found C 77.48, H 10.52, N 1.49, S 5.24.

Poly-4,5,9,10-tetrakis((2-ethylhexyl)oxy)pyrene-2,7-diyl-alt-(5,6-difluoro-4,7-di(thiophen-2-yl)- 2',1',3'-benzothiadiazole-5,5-diyl] (PP$_{EH}$-DTffBT): The titled product was synthesised as described previously in the preparation of **PP$_{HD}$-DTBT**. The product was obtained as a dark purple solid (30 mg, 24 %). GPC chloroform fraction: M_n = 5,300 Da; M_w = 6,300 Da; PDI = 1.18. ^{1}H NMR (500 MHz, $C_2D_2Cl_4$, 100°C): (δ_H/ppm) 8.85 (br.s, 4H), 8.50 (br.d, 2H), 7.82 (br.d, 2H), 4.3 (br.d, 8H), 2.05 (m, 4H), 1.94-1.27 (m, 32H), 1.14 (br.t, 12H), 0.98 (t, 12H). Elem. Anal. Calcd. For $C_{62}H_{76}F_2N_2O_4S_3$: C 71.09, H 7.31, N 2.67, S 9.18. Found C 62.00, H 6.40, N 2.60, S 9.00.

References

1   M. Willander, S. C. Jain and K. Vikram, 2007.

2   B. Fu, J. Baltazar, Z. Hu, A.-T. Chien, S. Kumar, C. L. Henderson, D. M. Collard and E. Reichmanis, *Chem. Mater.*, 2012, **24**, 4123–4133.

3   Z. B. Henson, K. Müllen and G. C. Bazan, *Nat. Chem.*, 2012, **4**, 699–704.

4   T. Xu and L. Yu, *Mater. Today*, 2014, **17**, 11–15.

5   P. P. Khlyabich, B. Burkhart, A. E. Rudenko and B. C. Thompson, *Polym. (United Kingdom)*, 2013, **54**, 5267–5298.

6   L. Lu, T. Zheng, Q. Wu, A. M. Schneider, D. Zhao and L. Yu, *Chem. Rev.*, 2015, **115**, 12666–12731.

7   I. H. Jung, D. Zhao, J. Jang, W. Chen, E. S. Landry, L. Lu, D. V Talapin and L. Yu, *Chem. Mater.*, 2015, **27**, 5941–5948.

8   H. Zhou, L. Yang, S. Stoneking and W. You, *ACS Appl. Mater. Interfaces*, 2010, **2**, 1377–1383.

9   H. Zhou, L. Yang and W. You, *Macromolecules*, 2012, **45**, 607–632.

10   A. Facchetti, *Mater. Today*, 2013, **16**, 123–132.

11   Y. Liu, J. Zhao, Z. Li, C. Mu, W. Ma, H. Hu, K. Jiang, H. Lin, H. Ade and H. Yan, *Nat. Commun.*, 2014, **5**.

12   N. Wang, Z. Chen, W. Wei and Z. Jiang, *J. Am. Chem. Soc.*, 2013, **135**, 17060–17068.

13   H. Yi, S. Al-Faifi, A. Iraqi, D. C. Watters, J. Kingsley and D. G. Lidzey, *J. Mater. Chem.*, 2011, **21**, 13649–13656.

14   Y. Wang, X. Xin, Y. Lu, T. Xiao, X. Xu, N. Zhao, X. Hu, B. S. Ong and S. C. Ng, *Macromolecules*, 2013, **46**, 9587–9592.

15   T. M. Figueira-Duarte and K. Müllen, *Chem. Rev.*, 2011, **111**, 7260–7314.

16   E. L. Williams, T. S. Ang, Z. Ooi, P. Sonar, T. T. Lin, W. T. Neo, J. Song and J. Hobley, *Polymers (Basel).*, 2014, **7**, 69–90.

17   P. Sonar, S. P. Singh, E. L. Williams, Y. Li, M. S. Soh and A. Dodabalapur, *J. Mater. Chem.*, 2012, **22**, 4425–4435.

18   A. B. Abdulaziz, *Chem. Commun.*, 2013, **49**, 2252–2254.

19   J. M. Casas-Solvas, J. D. Howgego and A. P. Davis, *Org. Biomol. Chem.*, 2014, **12**, 212–232.

20   N. Wang, X. Bao, Y. Yan, D. Ouyang, M. Sun, V. A. L. Roy, C. S. Lee and R. Yang, *J. Polym. Sci. Part A Polym. Chem.*, 2014, **52**, 3198–3204.

21   D. S. Yang, K. H. Kim, M. J. Cho, J. Jin and D. H. Choi, *J. Polym. Sci. Part A Polym.*

Chem., 2013, **51**, 1457–1467.

22   J.-H. Kim, H. U. Kim, I.-N. Kang, S. K. Lee, S.-J. Moon, W. S. Shin and D.-H. Hwang, *Macromolecules*, 2012, **45**, 8628–8638.

23   L. Cartwright, H. Yi and A. Iraqi, *New J. Chem.*, 2016.

24   L. Cartwright, A. Iraqi, Y. Zhang, T. Wang and D. G. Lidzey, *RSC Adv.*, 2015, **5**, 46386–46394.

25   L. Cartwright, L. J. Taylor, H. Yi, A. Iraqi, Y. Zhang, N. W. Scarratt, T. Wang and D. G. Lidzey, *RSC Adv.*, 2015, **5**, 101607–101615.

26   P. Patel, T. R. Hull, R. E. Lyon, S. I. Stoliarov, R. N. Walters, S. Crowley and N. Safronava, *Polym. Degrad. Stab.*, 2011, **96**, 12–22.

27   T. Umeyama, Y. Watanabe, E. Douvogianni and H. Imahori, *J. Phys. Chem. C*, 2013, **117**, 21148–21157.

28   Z. Li, J. Lu, S.-C. Tse, J. Zhou, X. Du, Y. Tao and J. Ding, *J. Mater. Chem.*, 2011, **21**, 3226–3233.

29   A. Misra, P. Kumar, R. Srivastava, S. K. Dhawan, M. N. Kamalasanan and S. Chandra, *Indian J. Pure Appl. Phys.*, 2005, **44**, 921–925.

30   J. Hu, D. Zhang and F. W. Harris, *J. Org. Chem.*, 2005, **70**, 707–708.

31   J. A. Letizia, S. Cronin, R. P. Ortiz, A. Facchetti, M. A. Ratner and T. J. Marks, *Chem. Eur. J.*, 2010, **16**, 1911–1928.

PPHD-DTBT

PPEH-DTBT

PPHD-DTffBT
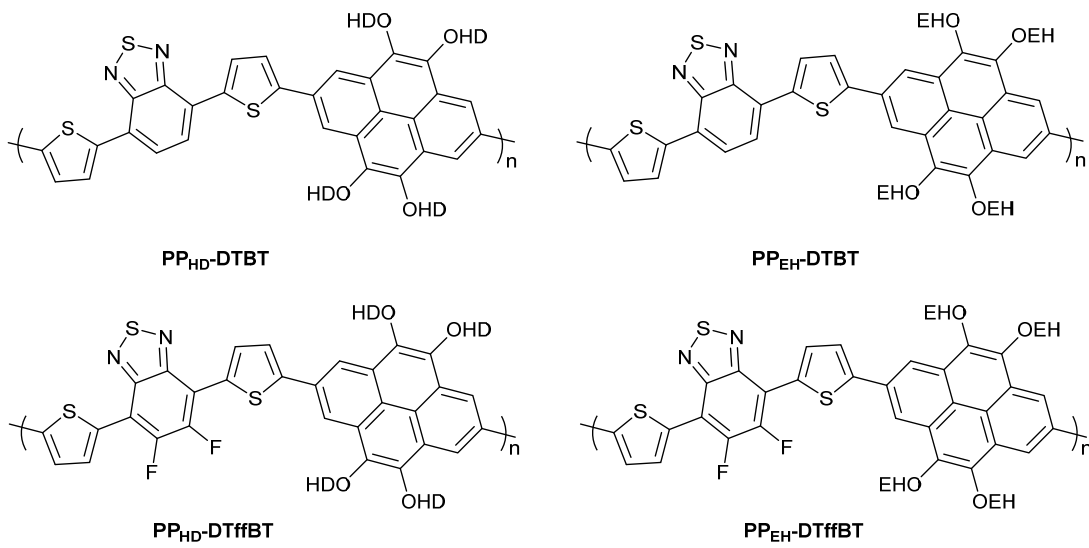
PPEH-DTffBT

Scheme 1: Polymer structures.

1 **2** **3** **4: R = 2-Hexyldecyl**
5: R = 2-Ethylhexyl
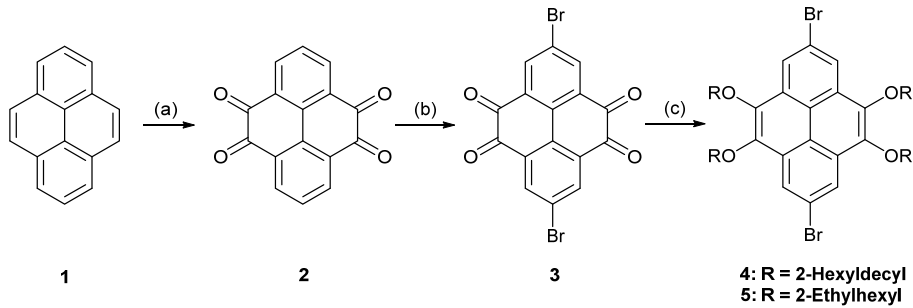
Scheme 2. (a) $RuCl_3 \cdot xH_2O$, $NaIO_4$, DCM, H_2O, MeCN; (b) NBS, H_2SO_4; (c) $Na_2S_2O_4$, n-Bu_4NBr, KOH, THF, H_2O, R-Br.

Table 1. GPC, UV-vis absorption and electrochemical data for **PPHD-DTBT**, **PPEH-DTBT**, **PPHD-DTffBT** and **PPEH-DTffBT**.

Polymer	M_n (Da)[c]	M_w (Da)[c]	PDI	λ_{max} (nm)		$E_{g\,opt}$ (eV)[d]	HOMO (eV)[e]	LUMO (eV)[f]	E_g^{elec} (eV)[g]
				Solution	Film				
PPEH-DTBT[a]	12,800	22,000	1.72	538	585	1.76	-5.45	-3.55	1.90
PPEH-DTffBT[a]	5,300	6,300	1.19	521	564	1.81	-5.53	-3.55	1.98
PPHD-DTBT[b]	20,500	30,200	1.47	531	571	1.79	-5.50	-3.28	2.22
PPHD-DTffBT[b]	20,700	40,400	1.95	526	562	1.84	-5.60	-3.28	2.32

[a] Measurements conducted on the chloroform fraction of the polymers. [b] Measurements conducted on the toluene fraction of the polymers. [c] GPC conducted in 1,2,4-trichlorobenzene at 140°C using a differential refractive index (DRI) method. [d] Optical band gap determined from the onset of the absorption band in thin film. [e] HOMO level determined from the onset of oxidation. [f] LUMO level determined from the onset of reduction. [g] Electrochemical band gap.
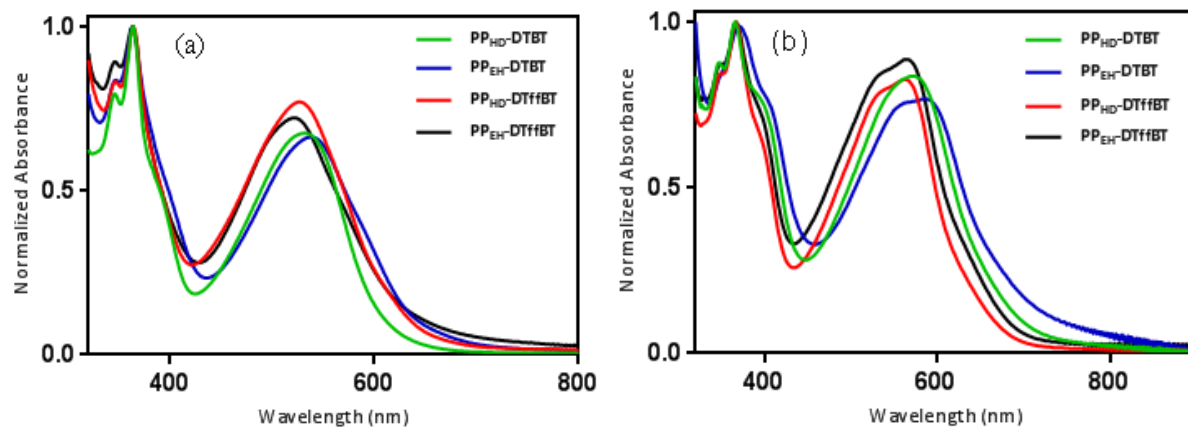
Figure 1. Normalised absorption spectra of **PP$_{HD}$-DTBT**, **PP$_{EH}$-DTBT**, **PP$_{HD}$-DTffBT** and **PP$_{EH}$-DTffBT** in: (*a*) chloroform solutions; and (*b*) thin films.
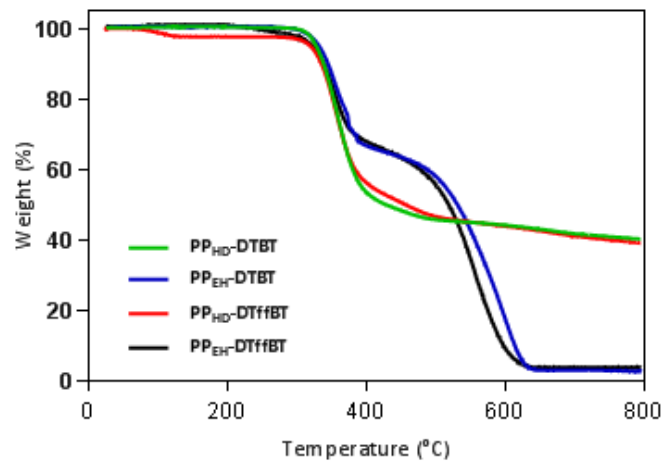
Figure 2: TGA curves of **PP$_{HD}$-DTBT**, **PP$_{EH}$-DTBT**, **PP$_{HD}$-DTffBT** and **PP$_{EH}$-DTffBT**.
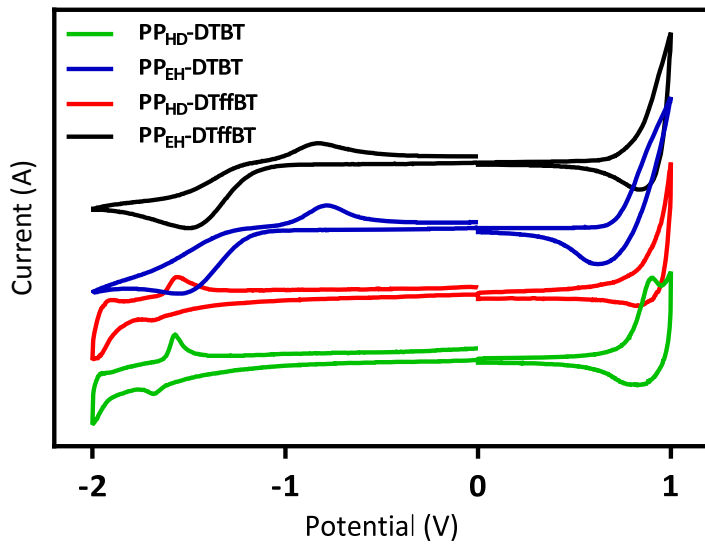
Figure 3. Cyclic voltammograms of thin films of **PP$_{HD}$-DTBT**, **PP$_{EH}$-DTBT**, **PP$_{HD}$-DTffBT** and **PP$_{EH}$-DTffBT** on platinum disc electrodes (area 0.031 cm^2) at a scan rate of 100 mV s^{-1} in acetonitrile / tetrabutyl ammonium perchlorate (0.1 mol dm^{-3}).
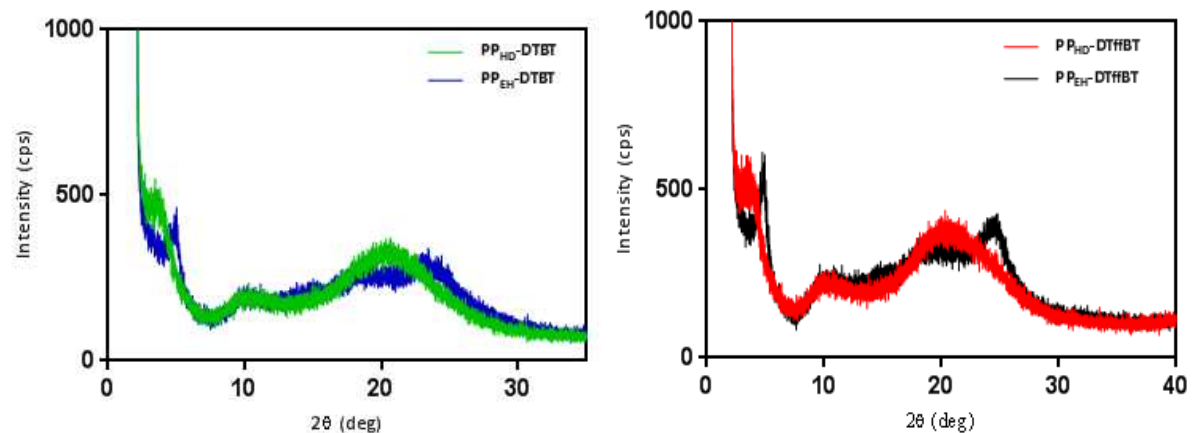

Figure 4. PXRD patterns of **PP$_{HD}$-DTBT**, **PP$_{EH}$-DTBT**, **PP$_{HD}$-DTffBT** and **PP$_{EH}$-DTffBT**.

Table 2. Device Performance of the four polymers **PP$_{HD}$-DTBT**, **PP$_{EH}$-DTBT**, **PP$_{HD}$-DTffBT** and **PP$_{EH}$-DTffBT**. Chlorobenzene was used as the processing solvent and all polymer:PC$_{70}$BM blend ratios were 1:3.

Polymer	J_{sc} (mA cm^{-2})	V_{oc} (V)	FF (%)	PCE (%)
PP$_{EH}$-DTBT	4.14	0.74	60.58	1.86
PP$_{EH}$-DTffBT	2.28	0.79	46.06	0.83
PP$_{HD}$-DTBT	2.38	0.90	45.81	0.98

| PP$_{HD}$-DTffBT | 1.36 | 0.93 | 52.22 | 0.66 |
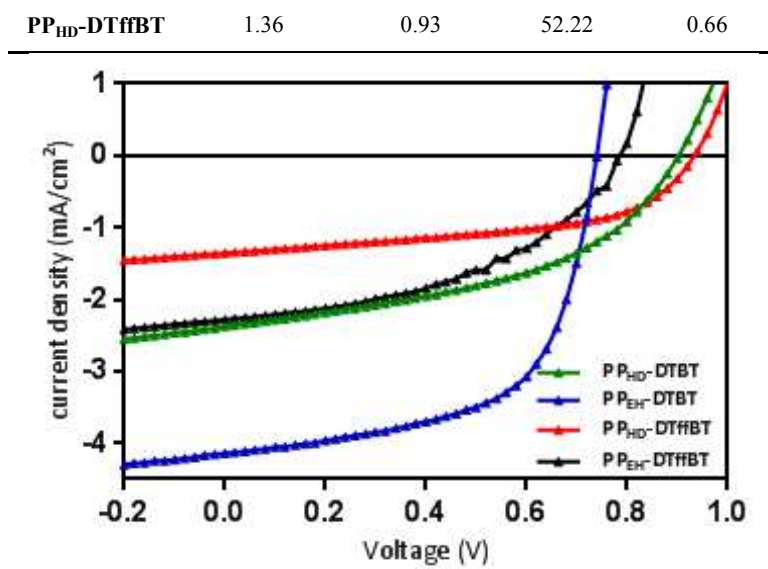
Figure 5. The J-V characteristic curves of **PP$_{HD}$-DTBT**, **PP$_{EH}$-DTBT**, **PP$_{HD}$-DTffBT** and **PP$_{EH}$-DTffBT.**